Numerical simulation of gas transport in aerogel pores



1998 J. Phys.: Condens. Matter 10 4947

(http://iopscience.iop.org/0953-8984/10/23/003)

J. Phys.: Condens. Matter **10** (1998) 4947–4953. Printed in the UK PII: S0953-8984(98)91810-0

# Numerical simulation of gas transport in aerogel pores

Anwar Hasmy†, Nathalie Olivi-Tran‡ and Rémi Jullien§

† Centro de Fısica, Instituto Venezolano de Investigaciones Cientıficas, Apartado 21827, Caracas 1020A, Venezuela

‡ Institut du Non Linéaire de Nice, 1361 route des Lucioles, Sophia-Antipolis, 06560 Valbonne, France

§ Laboratoire des Verres, Université Montpellier II, CC 069, place E Bataillon, 34095 Montpellier Cedex, France

Received 18 February 1998

**Abstract.** Gas permeability of aerogels was studied as a function of the aerogel concentration in non-densified and densified aerogels. To represent numerically the aerogel structure we have used the off-lattice diffusion-limited cluster–cluster–aggregation model which is a good model for base-catalysed aerogels. The sintering process is modelled by using a 'dressing' and 'contracting' process which has been previously introduced in the literature. A random ballistic motion of a gas particle inside the pores of the aerogels represents the gas motion. We also obtain a theoretical expression of the gas permeability as a function of the aerogel density.

## 1. Introduction

Aerogels are light porous materials which may be densified into silica glasses by a thermal process. In addition, these materials present a fractal structure which may be characterized by two typical lengths. The first is the average size of the fractal aggregates which compose the aerogel, and the second is the average size of the particles.

From a theoretical point of view, the diffusion-limited cluster–cluster–aggregation (DLCA) model [1, 2] provides a successful tool to numerically simulate the aerogel structure [3]. This model allows one to study the interaction of the fractal properties with several physical processes such as dynamic structure, i.e. vibrations of the structure [4], phase transition of pore confined materials [5] and densification [6, 7].

A scaling analysis showed that sintered aerogels preserve information concerning their original non-densified structure [8], and these findings have been confirmed by numerical models of the sintering process [6, 7].

Study of transport properties in porous systems is of fundamental interest and may have many applications. Fractal structure and permeability have been essentially studied in materials such as rocks and sand piles. As partially densified aerogels present a pore network correlation between two stages of sintering, they induce different properties in the permeability evolution during sintering than normally studied.

So, in this article, we study theoretically and numerically the gas permeability $K$ in sintered and non-sintered aerogels of different concentrations. As will be explained below, the gas transport is simulated by the random ballistic motion of a particle inside the pores of the aerogel. The present work is mainly focused on the gas permeability $K$ as a function of the aerogel concentration $c$. We develop a simple theory which leads to an expression which is able to reproduce the shape of the $K(c)$ numerical curves.

0953-8984/98/234947+07$19.50  

## 2. Numerical procedure

To build the original (non-sintered) aerogel structure, we have considered a three dimensional off-lattice diffusion-limited cluster–cluster–aggregation (DLCA) model [1, 2], which has already been extensively described elsewhere [9]. With this model we are able to obtain numerical aerogels of different concentrations.

To represent the aerogel sintering, we first use a coarsening process by dressing the structure. The sintered structure is obtained from the dressed structure after applying a proper homogeneous volume contraction which ensures mass conservation. In our case, we used the following procedure which has been introduced previously [7, 10]: all spherical particles composing the aerogel are dressed, and at stage $s$ of the sintering process, the dressed edge length $a_d$ of the particles becomes

$$a_d = a_0(1+s) \tag{1}$$

$a_0$ being the initial edge length of the particles. We compute the total volume $V_d(s)$ avoiding multiple counting of particles. The density of the partially densified aerogel (PDA) is then:

$$c(s) = \frac{V_d(s)}{(La_0)^3} \tag{2}$$

where $L$ is the edge length of the box containing the particles. Afterwards, one has to apply a 'contraction' factor ($\beta$) to the whole sample in order to have mass conservation:

$$\beta = \left(\frac{c(s)}{c_0}\right)^{1/3}. \tag{3}$$

Finally, the actual edge length $a_s$ of the particles (which is also called lower cut-off) in the sintered structure becomes:

$$a_s = \frac{a_d}{\beta} = a_0\frac{1+s}{\beta}. \tag{4}$$

Another interesting quantity to take into account is the specific surface area. The interface surface $S_d(s)$ of the dressed structure is simply related to the derivative of the function $V_d(s)$:

$$S_d(s) = 2\frac{V_d(s)}{da_d} = \frac{2}{a_0}\frac{\mathrm{d}V_d(s)}{\mathrm{d}s}. \tag{5}$$

In order to get the actual specific surface area $\Sigma(s)$, the above equation is divided by the total mass, and also by the appropriate scaling factor to get the expression:

$$\Sigma(s) = \frac{2}{a_0\rho_s}\frac{\mathrm{d}\log c(s)}{\mathrm{d}s}\beta(s) \tag{6}$$

where $\rho_s$ is the density of pure silica and $c(s)$ is the concentration of the sintered aerogel. For $s = 0$, in which case the structure is made of identical non-overlapping spheres, one obtains the exact result $a_0\rho_s\Sigma(0) = 6$ .

The numerical simulation of the gas motion proceeds as follows: initially a sphere of diameter $sa_0$ in the sintered aerogel ($a_0$ in the non-sintered case) is released at random inside the pores under the condition that it should not overlap with any other sphere (when $s$ and/or $c_0$ are too large many trials are necessary). Then, the sphere is allowed to follow a straight line motion in a chosen random direction (uniformly distributed in space) until it collides with a sphere of diameter $a_0$ in the aerogel. Immediately after collision a new random direction is selected (in a half space) according to the so-called Knudsen cosine law [11, 12], i.e. such that its probability distribution is proportional to $\cos\theta\mathrm{d}^2\Omega$ where $\theta$ is the angle

between this direction and the normal (centre-to-centre direction) and $d^2\Omega = \sin\theta d\theta d\phi$ is the elementary solid angle. In practice, $\theta$ is chosen such that $\cos^2\theta$ is uniformly distributed between zero and one, while the azimuthal angle is chosen uniformly between 0 and $2\pi$. It has been shown that this is essential to recover the equilibrium Boltzmann statistics and the right transport coefficients [11, 12]. Then, after a large number $N_c$ of collisions, and using periodic boundary conditions, one calculates the end-to-end square displacement $\ell^2$ of the diffusing sphere centre as well as the total length $\Lambda$ of its trajectory, which is the sum of the lengths of the successive segments. This allows us to calculate $D_d(s)$ by the well known formula:

$$D_d(s) = \frac{1}{6} v \frac{\ell^2}{\Lambda} \tag{7}$$

where $v$ $(= \sqrt{8kT/\pi m})$ is the mean molecular velocity of the gas particle of mass $m$ at temperature $T$. To calculate the gas permeability $K(s)$, which is the ratio between the gas flux through the sintered material and the applied pressure gradient, we have used the fact that it is simply related to the gas diffusion constant $D_s(s)$ inside the pores by

$$K(s) = (1 - c(s))D_s(s). \tag{8}$$

Introducing the gas diffusion constant inside the pores of the dressed structure $D_d(s) = \beta(s)^2 D_s(s)$, this formula becomes:

$$K(s) = \frac{1 - c(s)}{\beta(s)^2} D_d(s). \tag{9}$$

Since the experimental situation that we would like to describe corresponds to low pressures and small gas particles (smaller than silica particles), the diffusion constant $D_d(s)$ is related to the Knudsen motion of a point particle inside the pores of the dressed structure. For the sintered case, given the dressed structure, characterized by the box size $L$, $c_0$ and $s$, we have indirectly computed $D_d(s)$ by allowing a hard sphere of diameter $sa_0$ to perform a Knudsen motion inside the voids of the undressed (non-sintered) structure made of spheres of diameter $a_0$. Such a device has already been used elsewhere [13].

## 3. Theory

Since $D \propto \ell^2/\Lambda$ (see equation (7)), theoretical estimation of the diffusion coefficient for a given aerogel of concentration $c$ requires knowledge of the end-to-end square displacement as well as the total length of the trajectory.

One may approximate $\ell^2$ by the characteristic length due to the mean size of the pores:

$$\ell^2 \propto (1 - c)^{2/3}. \tag{10}$$

Then, $\Lambda$ may be computed by assuming that the number of collisions with the walls of the pores is directly proportional to its specific surface, so that:

$$\Lambda \propto \frac{(1 - c)^{1/3}}{\Sigma} \tag{11}$$

which can be considered as a mean free path.

From a dimensional point of view, this former relation is not exact except if we take $\Sigma$ as a probability. Indeed, it would be more precise to write:

$$\Lambda \propto \frac{(1 - c)^{1/3}}{\Sigma/\Sigma_0} \tag{12}$$

where $\Sigma_0$ is the specific surface of the less dense aerogel (for the non-sintered aerogel case), or the initial specific surface for sintered aerogels. Finally, we obtain that the diffusion constant varies as:

$$D \propto (1-c)^{1/3}\Sigma. \tag{13}$$

For a non-sintered aerogel, we take into account that $c\Sigma \propto cte$ [10], which combined with relation (13) leads to:

$$D \propto \frac{(1-c)^{1/3}}{c}. \tag{14}$$

From equation (8) and the above expression one obtains the following relation for the gas permeability:

$$K \propto \frac{(1-c)^{4/3}}{c}. \tag{15}$$

For sintered aerogels, the formula is slightly different. In this second case, we introduce in the above scaling argument the contraction factor [8], which behaves as:

$$\beta \propto c(s)^{1/3}. \tag{16}$$

The specific surface (equation (6)) becomes:

$$\Sigma \propto \frac{\mathrm{d}\log c}{\mathrm{d}s}\beta(s). \tag{17}$$

Knowing that the permeability of the sintered structure is:

$$K \propto \frac{(1-c(s))}{\beta(s)^2}D(s) \tag{18}$$

and according to equation (1), the final expression for the permeability in the sintered aerogel gives:

$$K(s) \propto \frac{(1-c(s))^{4/3}}{c(s)^{1/3}}\frac{\mathrm{d}\log c}{\mathrm{d}s}. \tag{19}$$

## 4. Results

In figure 1, we compare the numerical behaviour (symbols) of the permeability $K$ as a function of the concentration $c$ for non-sintered aerogels with the curve corresponding to the theoretical scaling relation (15) (solid curve). The numerical results have been obtained by averaging 60 independent simulations.

Figure 2 illustrates the numerical behaviour of the permeability $K$ as a function of the concentration $c$ for sintered aerogels. The solid curve corresponds to relation (19), while the symbols correspond to numerical data which result from an average of 100 independent simulations. Here, as in figure 1, we note the remarkable agreement between theory and simulation. In both figures 1 and 2 the theoretical curve has been shifted vertically for convenience.

Gas permeability experiments on partially densified aerogels have been performed by Beurroies *et al* [14] using a newly designed apparatus which allows simultaneous measurement of the gas flux through a cylindrical sample and the gas pressure difference between the two edges. Two series of experimental data published elsewhere [14] have been considered here for comparison with our results, each one corresponding to different gases: nitrogen and argon. In figure 3 we compare our numerical $K(c)$ results in sintered

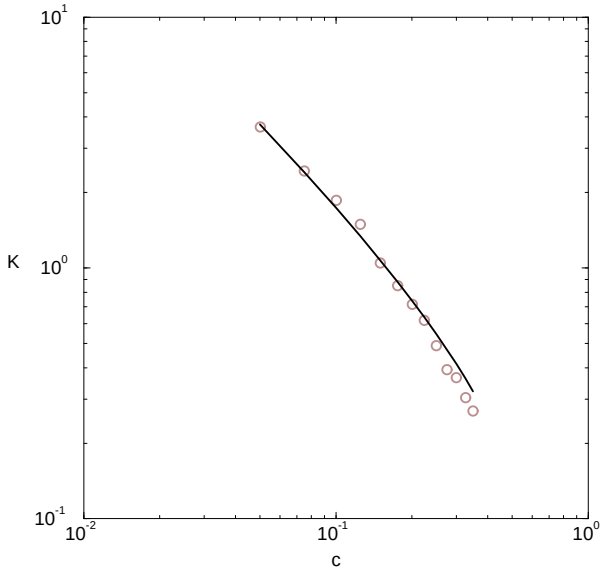


**Figure 1.** Log–log plot of $K$ versus $c$ for non-sintered aerogels. The solid line corresponds to the theoretical curve and symbols to the numerical data. The numerical curve results from an average of 60 independent simulations for each aerogel concentration.

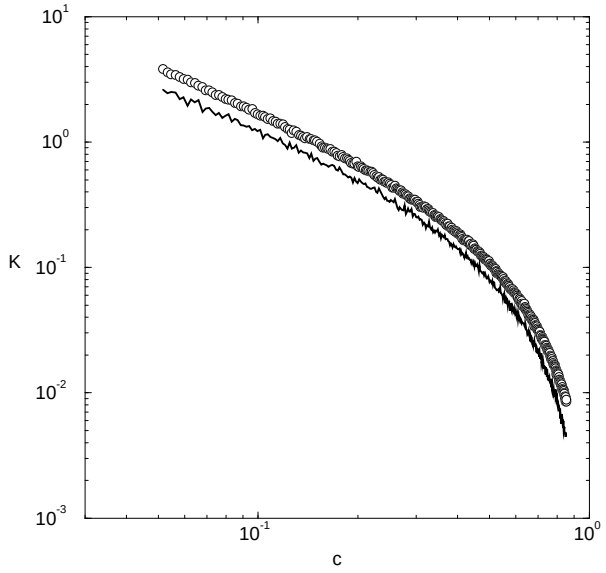


**Figure 2.** Log–log plot of $K$ versus $c$ for sintered aerogels. The solid line corresponds to the theoretical curve and symbols to the numerical data. For the numerical calculations we considered $c_0 = 005$ and $L = 577$. Numerical results has been obtained of an average of 100 independent simulations for each aerogel concentration.

aerogels to experimental data corresponding to a series of partially densified aerogels which have been prepared under neutral conditions. Before sintering, their density is known to be equal to $\rho_0 = 0.25$ g cm$^{-3}$. Note that, after dividing by the gas velocity, and normalizing

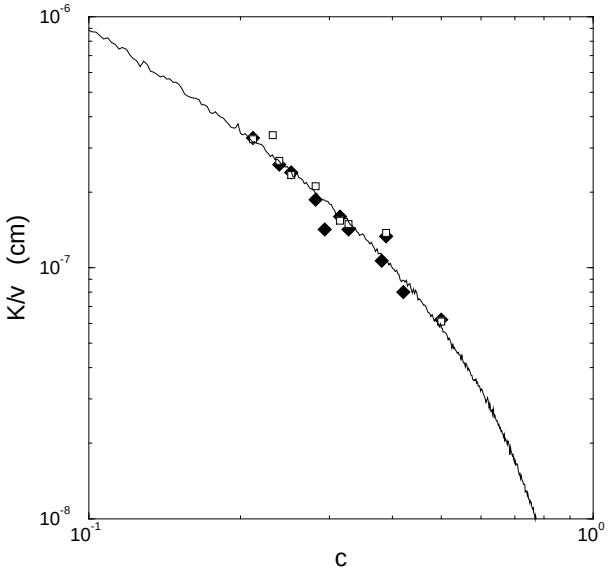


**Figure 3.** Comparison of the numerical $K(c)$ curve reported in figure 2, with experimental data of the normalized experimental permeability $K/v$ for neutral PDA aerogels. Squares and diamonds correspond to argon and nitrogen, respectively.

adequately the $K(c)$ numerical curve, the experimental (symbols) and the numerical curves (solid curve) in both cases coincide.

## 5. Discussion

In the above results, as expected, the permeability $K$ decreases when the aerogel concentration $c$ increases. For the sintered case (figure 2), the permeability curve has non-trivial behaviour near a concentration approximately equal to 0.8. Indeed, this concentration can be interpreted as a percolation pores threshold, i.e. a concentration where the gas particle cannot percolate from one side to the opposite side of the aerogel. Near this concentration, the closed pores in the aerogels are very numerous. Unfortunately, for non-sintered numerical aerogels it is very hard to obtain high concentrations, so the study of this region of concentrations remains open.

Prior work by Olivi-Tran and Jullien [6] showed that if one takes an initial non-sintered aerogel of very low concentration, its pores tend to close at very high concentration: for an initial concentration $c_0 = 0.05$, all the pores are closed for a sintered concentration near $c(s) = 0.95$. So at the beginning of the computation, i.e. for low concentration, the computed gas particle has a very low probability to begin its walk in a closed pore, situation that is closest to experiments.

The behaviour observed in figure 2 near the percolation region denotes that simple scaling ideas can not be applied here. One should not be surprised if parameters characterizing the system behave with a set of critical exponents, since the percolation phenomenon is a typical example of a phase transition phenomenon. In fact, the quick decreasing in $c$ may reflect, in some manner, the divergence of the correlation length, which in this case is associated with increasing characteristic pore size when aerogel concentration decreases.

Experimental data (figure 3) reinforce our theoretical and numerical model as they agree very well with the latter.

## 6. Conclusion

We have introduced an expression which is able to reproduce numerical data of the gas permeability as a function of the aerogel concentration. For both sintered and non-sintered aerogels the agreement between theory and simulation is remarkable. A similar shape of the permeability curves has been also observed in experiments. In addition, for the sintered case we found a non percolation regime for the gas inside the pore of the aerogel. In this case, a small discrepancy between theory and simulation at high aerogel concentrations suggests that our theoretical approach does not take into account effects such as the expected phase transition from percolation to non-percolation of pores. In this limit we believe that typical critical exponents should not be neglected.

## References

[1] Meakin P 1983 *Phys. Rev. Lett.* **51** 1119
[2] Kolb M, Botet R and Jullien R 1983 *Phys. Rev. Lett.* **51** 1123
[3] Hasmy A, Foret M, Anglaret E, Pelous J, Vacher R and Jullien R 1995 *J. Non-Cryst. Solids* **186** 118
[4] Thouy R, Jullien R and Benoit C 1995 *J. Phys.: Condens. Matter* **7** 9703
[5] Uzelac K, Hasmy A and Jullien R 1995 *J. Non-Cryst. Solids* **186** 365
[6] Olivi-Tran N and Jullien R 1995 *Phys. Rev.* B **52** 258
[7] Jullien R, Olivi-Tran N, Hasmy A, Woignier T, Phalippou J, Bourret D and Sempéré R 1995 *J. Non-cryst. Solids* **188** 1
[8] Sempéré R, Bourret D, Woignier T, Phalippou J and Jullien R 1993 *Phys. Rev. Lett.* **71** 3307
[9] Hasmy A, Anglaret E, Foret M, Pelous J and Jullien R 1994 *Phys. Rev.* B **50** 6006
[10] Hasmy A, Beurroies I, Bourret D and Jullien R 1995 *Europhys. Lett.* **29** 567
[11] Levitz P 1993 *J. Chem. Phys.* **97** 3813
[12] Walleau J P, Diestler D, Cushman J H, Schoen M, Hertzner A and Riley M E 1991 *J. Chem. Phys.* **95** 6194
[13] Torquato S 1991 *J. Chem. Phys.* **95** 2838
[14] Beurroies I, Bourret D, Sempéré R and Phalippou J 1995 *J. Non-Cryst. Solids* **186** 328